



Superstructure phase of microwave dielectric $(\text{Bi}_{1.5}\text{Zn}_{0.5})(\text{Ti}_{1.5}\text{Nb}_{0.5})\text{O}_7$ pyrochlore

Y. Liu, R.L. Withers and T.R. Welberry

Research School of Chemistry, The Australian National University, ACT 0200, Australia

The cubic $Fd\bar{3}m$ pyrochlore $(\text{Bi}_{1.5}\text{Zn}_{0.5-\alpha})(\text{Zn}_{0.5}\text{Nb}_{1.5})\text{O}_{7-\alpha}$ (BZN) and related Bi based pyrochlores are attractive candidate materials for use in future wireless communications technology as a result of their high (and tuneable) dielectric constants and low dielectric losses in the RF/microwave frequency range coupled with their relatively low sintering temperatures. In the case of $(\text{Bi}_{1.5}\text{Zn}_{0.5})(\text{Ti}_{1.5}\text{Nb}_{0.5})\text{O}_7$ (BZTN), the continuous $\mathbf{G} \pm \langle 10l \rangle^*$ type diffuse streaking characteristic of the BZN-related pyrochlores has virtually condensed out to give relatively sharp $\mathbf{G} \pm \langle 001 \rangle^*$ "satellite reflections" and a P4₃32, close to a superstructure, phase of average pyrochlore unit cell dimensions. Bond valence sum considerations are used to investigate the local crystal chemistry of this BZNT phase and to derive a plausible model for the superstructure phase. The additional $\mathbf{G} \pm \langle 001 \rangle^*$ satellite reflections are due to short range ordering of Bi and Zn ions on the A sites of the O'A₂ sub-structure of the pyrochlore average structure type coupled with associated strain induced structural relaxations.

1. Introduction

Bi-based pyrochlore phases such as $(\text{Bi}_{1.5}\text{Zn}_{0.5-\delta})(\text{Zn}_{0.5}\text{Nb}_{1.5})\text{O}_{7-\delta}$ (BZN) have been the subject of much recent interest as a result of their relatively low sintering temperatures and often excellent dielectric properties including electric field tuneability. The inherent disorder of these Bi-based, $A_2B_2O_7$ (or $B_2O_6 \cdot O'A_2$) pyrochlore systems is of some interest as it is believed to be strongly correlated with their dielectric relaxation properties [1-4]. We have recently found clear evidence (in the form of highly structured, $\mathbf{G} \pm \langle 10l \rangle^*$ type diffuse scattering [\mathbf{G} a Bragg reflection of the underlying $Fd\bar{3}m$ average structure] observed via electron diffraction) for short range ordering of Bi and Zn metal ions on the A site positions of the O'A₂ sub-structure of the ideal pyrochlore structure type in the case of BZN. The local Bi/Zn compositional ordering and associated displacive disorder responsible was qualitatively interpreted via Monte Carlo modelling guided by the insights provided by a bond valence sum analysis of the average crystal structure and showed that each of the constituent O'A₄ tetrahedra making up the O'A₂ sub-structure must have O'Bi₃Zn stoichiometry [5]. This paper extends the results of our previous work to a new, Bi-based pyrochlore superstructure phase *i.e.* $(\text{Bi}_{1.5}\text{Zn}_{0.5})(\text{Ti}_{1.5}\text{Nb}_{0.5})\text{O}_7$ (BZTN).

2. Sample preparation

$(\text{Bi}_{1.5}\text{Zn}_{0.5})(\text{Ti}_{1.5}\text{Nb}_{0.5})\text{O}_7$ (BZTN) was synthesized by solid state reaction from high purity oxide starting materials. The powders were homogeneously mixed and then annealed for several days at 1050°C. Samples suitable for Transmission Electron Microscope (TEM) were prepared by the dispersion of finely ground material onto a holey carbon film. Electron Diffraction Patterns (EDP's) were obtained with a Philips EM 430 TEM.

3. Results and Discussion

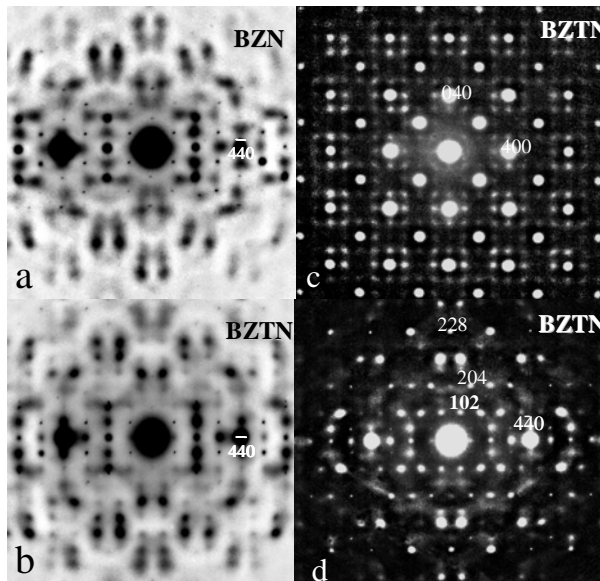


Fig.1 Typical $\sim \langle 551 \rangle$ zone axis EDP's of (a) BZN and (b) BZTN as well as (c) $\langle 001 \rangle$ and (d) $\langle 221 \rangle$ zone axis EDP's of BZTN.

Fig.1 shows typical $\sim \langle 551 \rangle$ zone axis electron diffraction patterns (EDP's) of (a) BZN and (b) BZTN as well as (c) $\langle 001 \rangle$ and (d) $\langle 221 \rangle$ zone axis EDP's of BZTN. Similar EDP's were always observed for both BZN and BZTN (*c.f.* for example Fig.1a with Fig.1b). Thus the same short range chemical ordering of the Bi and Zn ions on the ideal pyrochlore A site positions (along with the associated structural relaxation) must again be largely responsible for the observed structured diffuse distribution [5]. There is a difference however. The extended $G \pm \langle 10l \rangle^*$ type diffuse streaking along the $\langle 001 \rangle^*$ directions of reciprocal space in the case of BZN appear to have largely condensed into $G \pm \langle 100 \rangle^*$ 'satellite reflections' in the case of

BZNT *e.g.* the 'reflection' labelled $[102]^*$ in Fig.1d = $[002]^* + [100]^*$ *etc.* is not an allowed Bragg reflection of the $Fd\bar{3}m$ average pyrochlore structure type. Note that the resultant superstructure is of average pyrochlore unit cell dimensions and necessarily *P*-centred.

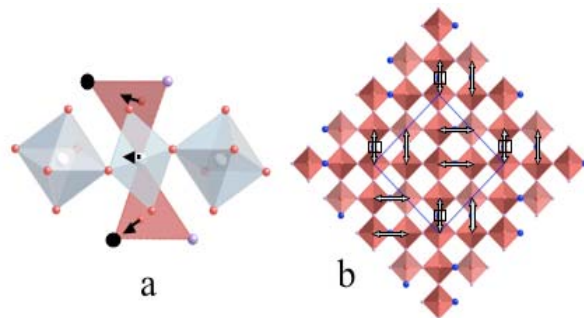


Fig.2 (a) The hexagonal prismatic environment of the A cations in the pyrochlore average structure type in projection along $\langle 1, -1, 0 \rangle$ and (b) an $\langle 001 \rangle$ projection of the $O'A_2$ tetrahedral sub-structure of the ideal pyrochlore structure type. The Zn ions are represented by the larger black balls in (a) and blue balls in (b). The Bi ions are represented by the pink balls in (a) and (b). A possible Bi/Zn ordering pattern with an overall space group symmetry of $P4_332$ is shown in (b).

We begin by assuming that each $O'A_4$ tetrahedron of the ideal $O'A_2$ sub-structure (see Fig.2b) has $O'Bi_3Zn$ stoichiometry, as is the case for BZN. Given this, here are only two possible types of inter-tetrahedral Zn-Zn separation distances. The first is of $\frac{1}{4} \langle 112 \rangle$ type as shown in Fig.2a. Because the Zn ions are $\sim 50\%$ underbonded in the average structure type, neighbouring O' ions centring the $O'Bi_3Zn$ tetrahedra must shift directly in towards the Zn ions. The Bi ions in the same tetrahedra cannot afford to lose the valence contribution from these O' ions, however, and will seek to follow the induced O' ion shifts. This induces shifts of the Bi ions perpendicular to the local $O'-Bi-O'$ axis towards two of the six surrounding equatorial O ions (see Fig.2a). The only other possible type of

inter-tetrahedral Zn-Zn separation distance is $\frac{1}{2} \langle 110 \rangle$. Such a Zn-Zn separation distance, however, does not allow the Bi ions to follow the O' shifts and leads to a significantly under-



bonded Bi ion. It is therefore energetically extremely unfavourable and does not occur. This provides a crystal chemical rationale for why $1/4$ $\langle 112 \rangle$ type Zn-Zn separation distances are strongly favoured and $1/2$ $\langle 110 \rangle$ type Zn-Zn separation distances completely avoided in BZN-related pyrochlores.

Applying these ordering principles and assuming a 'marker' Zn ion at $1/8, 1/8, 1/8$ (marked by the open squares in Fig.2b) there are two only Bi/Zn ordering patterns compatible with a P -centred resultant superstructure of average pyrochlore unit cell dimensions. The first, shown in Fig.2b above, has resultant $P4_332$ space group symmetry while the symmetry related second, has resultant $P4_132$ space group symmetry. The Zn ions are represented by the larger blue balls at the corners of the $O'Bi_3Zn$ tetrahedra while the O' -Zn- O' "zincanyl" type units are marked by the double-headed arrows. Note that the characteristic arrangement of the O' -Zn- O' "zincanyl" type units completely destroys the original face-centring symmetry operations of the underlying pyrochlore type average structure. Relatively extended distributions of this type must occur in the case of BZNT in order to account for the sharpness of the observed "satellite reflections" (see *e.g.* Fig.1).

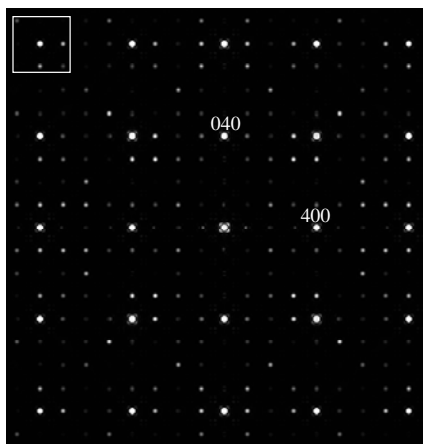


Fig.3 A Monte Carlo simulated $\langle 001 \rangle$ EDP based on the above model for comparison with Fig.1c.

Following the principles enunciated above, a fully ordered model structure for BZNT in space group $P4_332$, $a = 10.3528 \text{ \AA}$, has been derived. In order to confirm this, Monte Carlo simulation (see [5,6] for details) was used to produce a 'size effect' relaxed $O'Bi_{1.5}Zn_{0.5}$ distribution starting with the undistorted $O'Bi_{1.5}Zn_{0.5}$ distribution of space group symmetry $P4_332$ shown in Fig.2b. Fig.3 shows the corresponding simulated $\langle 001 \rangle$ type diffraction pattern using this distribution. A good qualitative agreement (*cf. e.g.* the relative intensities of the satellite reflections around the $[\bar{8}80]^*$ pyrochlore Bragg reflection contained within the white box of Fig.3 and Fig.1c and confirms the plausibility of the proposed structural model.

Acknowledgments

YL and RLW acknowledge financial support from the Australian Research Council (ARC) in the form of an ARC Discovery Grant.

References

1. G.H. Haertling and C.E. Land, *J. Am. Ceram. Soc.* **54**, 1 (1971).
2. J. Ravez and A. Simon, *Eur. Phys. J.* **AP11**, 9 (2000).
3. P. Sciau, Z. Lu, G. Galvarin, T. Roisnel and J. Ravez, *Mat. Res. Bull.* **28**, 1233 (1993).
4. H. El Alaoui-Belghiti, A. Simon, M. Elaammani, J.M. Reau and J. Ravez, *Phys. Status Solidi B*, in press.
5. R.L. Withers, T.R. Welberry, A.-K. Larsson, Y. Liu, L. Norén, H. Rundlöf, and F.J. Brink, *J. Solid State Chem.* **177**, 231 (2004).
6. Y. Liu, R.L. Withers, T.R. Welberry, H. Wang and H. Du, *J. Solid State Chem.* **179**, 231 (2006).